Cell, Vol. 120, 831–842, March 25, 2005, Copyright ©2005 by Elsevier Inc. DOI 10.1016/j.cell.2005.01.012

SREBP Pathway Responds to Sterols and Functions as an Oxygen Sensor in Fission Yeast

Adam L. Hughes,[1] Bridget L. Todd,[1] and Peter J. Espenshade[1,*]
[1]Department of Cell Biology
Johns Hopkins University School of Medicine
Baltimore, Maryland 21205

Summary

Cholesterol and fatty acid synthesis in mammals are controlled by SREBPs, a family of membrane bound transcription factors. Our studies identified homologs of SREBP, its binding partner SCAP, and the ER retention protein Insig in *Schizosaccharomyces pombe*, named *sre1*$^+$, *scp1*$^+$, and *ins1*$^+$. Like SREBP, Sre1 is cleaved and activated in response to sterol depletion in a Scp1-dependent manner. Microarray analysis revealed that Sre1 activates sterol biosynthetic enzymes as in mammals, and, surprisingly, Sre1 also stimulates transcription of genes required for adaptation to hypoxia. Furthermore, Sre1 rapidly activates these target genes in response to low oxygen and is itself required for anaerobic growth. Based on these findings, we propose and test a model in which Sre1 and Scp1 monitor oxygen-dependent sterol synthesis as an indirect measure of oxygen supply and mediate a hypoxic response in fission yeast.

Introduction

Lipid homeostasis in mammalian cells is controlled by a family of ER membrane bound transcription factors called sterol regulatory element binding proteins (SREBPs) (Rawson, 2003). Two genes code for three SREBP isoforms, named SREBP-1a, SREBP-1c, and SREBP-2. To date, SREBPs are known to activate transcription of more than 30 genes needed for uptake and synthesis of cholesterol, fatty acids, triglycerides, and phospholipids (Horton et al., 2002). Activity of SREBPs is regulated by sterol feedback inhibition, with SREBP being active in sterol-depleted cells and inactive when cholesterol accumulates.

SREBPs contain two transmembrane segments and are inserted into ER membranes in a hairpin fashion such that the N- and C-terminal ends of the protein project into the cytosol (Figure 1A). The SREBP N terminus is a transcription factor of the basic helix-loop-helix-leucine zipper (bHLH-zip) family, and the C terminus binds to the C terminus of SREBP cleavage activating protein, SCAP (Rawson, 2003). SCAP is an ER membrane protein that contains eight transmembrane segments and is a component of the sterol sensor (Figure 1B). Cells containing mutations in the sterol-sensing domain (SSD, transmembrane segments 2–6) of SCAP fail to sense sterols, resulting in activation of SREBP even in the presence of high sterol levels (Yabe et al., 2002).

*Correspondence: peter.espenshade@jhmi.edu

SREBP is activated by two sequential proteolytic cleavage events in the Golgi (Rawson, 2003). Sterols control activation of SREBP by regulating access of SREBP to the Golgi-localized Site-1 and Site-2 proteases. In sterol-replete cells, SCAP forms a complex with the ER resident protein Insig (Yang et al., 2002). As a result, ER exit of SREBP-SCAP complex is blocked, preventing activation of SREBP. In sterol-depleted cells, SCAP escorts SREBP from the ER to the Golgi where the Site-1 and Site-2 proteases cleave SREBP and release the N-terminal transcription factor (DeBose-Boyd et al., 1999). How SCAP and Insig function to sense sterols is unknown.

To date, SREBP homologs have been characterized in two model genetic organisms, *D. melanogaster* and *C. elegans*. Both organisms are sterol auxotrophs and thus do not regulate sterol synthesis (McKay et al., 2003; Seegmiller et al., 2002). Consequently, SREBP only regulates genes required for fatty acid synthesis in these organisms. Furthermore, while *Drosophila* SREBP is activated by an orthologous SCAP-dependent mechanism, cleavage of dSREBP is regulated by levels of phosphatidylethanolamine, not sterols (Dobrosotskaya et al., 2002). In contrast, yeast synthesize ergosterol, a sterol structurally similar to cholesterol. We therefore postulated that yeast may possess an SREBP pathway to regulate ergosterol homeostasis.

In this study, we present the characterization of an SREBP pathway in a unicellular eukaryote, the fission yeast *S. pombe*. We demonstrate that *sre1*$^+$ and *scp1*$^+$ are functional orthologs of SREBP and SCAP and that yeast activate Sre1 in response to sterol depletion. Surprisingly, *sre1*$^+$ is essential only for anaerobic growth, and *sre1*$^+$ regulates genes required for adaptation to hypoxia. Our data support a model whereby in low oxygen, the Sre1-Scp1 complex senses a decrease in oxygen-dependent sterol synthesis, leading to proteolytic activation of Sre1 and transcriptional adaptation to hypoxia. We therefore propose that Sre1-Scp1 function as an oxygen sensor in fission yeast.

Results

SREBP Pathway in Fission Yeast

Sequence searches failed to identify a SREBP homolog in *S. cerevisiae*, but two genes homologous to human SREBP-1a, *sre1*$^+$ and *sre2*$^+$, were identified in the fission yeast *S. pombe* (Figure 1A). Despite low overall sequence identity to SREBP-1a, the N-terminal domains of Sre1 and Sre2 contain basic bHLH-zip DNA binding domains with high identity to the SREBP-1a bHLH domain, 59% and 63% for Sre1 and Sre2, respectively. Importantly, Sre1 and Sre2 contain a unique tyrosine residue in the bHLH domain that distinguishes SREBPs from other bHLH transcription factors (Parraga et al., 1998). Like mammalian SREBPs, the N termini of Sre1 and Sre2 are serine- and proline-rich, with these amino acids comprising 32% and 27%, respectively, of residues preceding the bHLH domain (Hua et al., 1993).

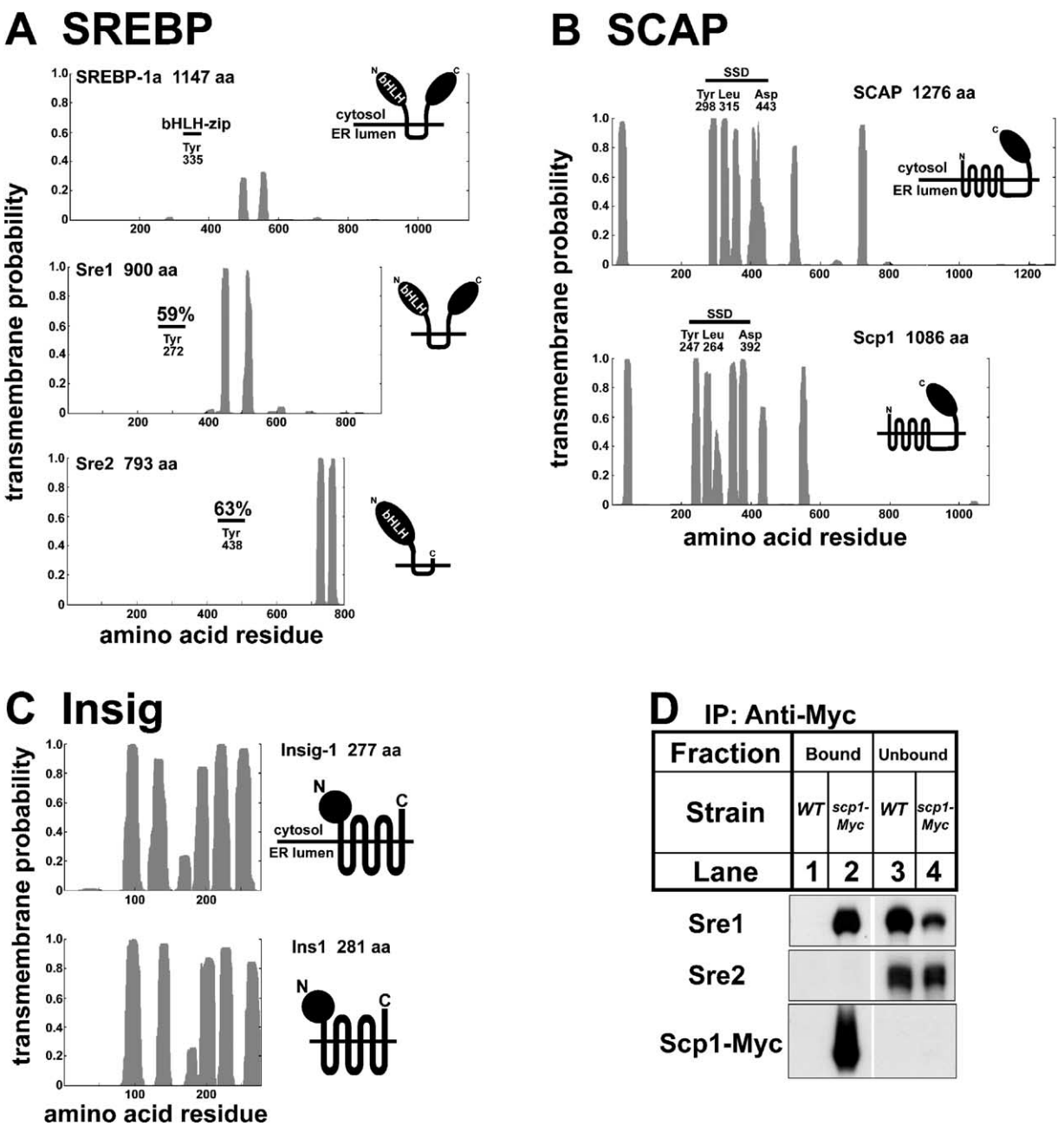

Figure 1. *S. pombe* Homologs of Mammalian SREBP, SCAP, and Insig

Transmembrane helix prediction plots of human SREBP-1a (A), hamster SCAP (B), and human Insig-1 (C) calculated using TMHMM software (version 2.0) are shown in comparison to their *S. pombe* homologs. Protein lengths are given in amino acids (aa). Heavy bars indicate regions of high sequence identity. For SREBP, the amino acid position of the highly conserved tyrosine in the bHLH zipper domain (bHLH-zip) is given. For SCAP, the positions of three conserved residues in the sterol-sensing domain (SSD) that confer constitutive activity on SCAP are shown (Yabe et al., 2002). Predicted membrane topology is diagrammed (not to scale) for each protein. ORF designations are as follows: *sre1*$^+$, SPBC19C2.09; *sre2*$^+$, SPBC354.05c; *scp1*$^+$, SPBC3B9.15c; and *ins1*$^+$, SPCC306.05c. (D) Wild-type or *scp1-Myc* yeast (3×10^7 cells) were harvested, and detergent-solubilized extracts were prepared as described in Experimental Procedures. Proteins associated with Scp1-Myc were immunopurified using anti-Myc IgG-9E10 monoclonal antibody. Equal fractions of bound (lanes 1 and 2) and unbound (lanes 3 and 4) protein were subjected to immunoblot analysis using anti-Sre1(aa 1–260) IgG, anti-Sre2 (aa 1–426) serum, or anti-Myc IgG-Poly as indicated.

Sre1 and Sre2 are predicted to contain two transmembrane helices, suggesting that these proteins are membrane bound transcription factors with a topology similar to mammalian SREBP. Interestingly, while Sre1 and Sre2 share overall topology, Sre2 lacks the C-terminal SCAP-interacting domain found in mammalian SREBPs.

Fission yeast also contains a single homolog of SCAP that we named *scp1*$^+$ (Figure 1B). Both mamma-

lian SCAP and fission yeast Scp1 are predicted to contain eight transmembrane helices and a large C-terminal domain with multiple WD repeats (Smith et al., 1999). Membrane helices 2–6 of SCAP comprise the sterol-sensing domain (SSD) that controls activation of SREBP in response to sterol levels. Previous studies identified three amino acids in the SSD of SCAP required for binding to Insig and retention in the ER: Tyr298, Leu315, and Asp443 (Yabe et al., 2002). Mutation of these residues causes the SREBP-SCAP complex to exit the ER constitutively, regardless of sterol concentration. Importantly, despite the fact that SCAP and Scp1 share little overall sequence identity, patches of identity surround these three conserved residues in the Scp1 SSD (Tyr247, Leu264, Asp392), suggesting that Scp1 may sense sterols in yeast.

Lastly, database searches revealed a sequence homolog of human Insig-1 that we named *ins1*$^+$ (Figure 1C) (Loewen and Levine, 2002). Overall sequence identity between the two proteins is low (21%), but the proteins are nearly identical in length and predicted topology. Based on a recent characterization of Insig-1, Ins1 also likely contains six transmembrane segments (Feramisco et al., 2004).

To test whether Scp1 and Sre1 form a complex, we constructed *scp1-Myc*, a yeast strain that expresses Scp1 with a C-terminal 13xMyc tag from the endogenous *scp1*$^+$ promoter. We purified Scp1 complexes from wild-type and *scp1-Myc* detergent cell extracts using anti-Myc antibody, and equal amounts of bound and unbound fractions were analyzed. Immunoblotting with antibody to the N terminus of Sre1 shows that greater than 50% of endogenous Sre1 is bound to Scp1-Myc (Figure 1D, upper panel, lanes 2 and 4). No Sre1 was recovered from wild-type cells that lack the Myc epitope (Figure 1D, lane 1). To test the specificity of Scp1-Sre1 binding, we probed the same samples with antibody to the N terminus of the closely related Sre2. Scp1-Myc failed to bind to Sre2 (Figure 1D, middle panel, lane 2), likely due to the absence of a Scp1-interacting domain in Sre2. These data demonstrate that Scp1 and Sre1 form a complex in fission yeast.

To investigate whether Sre1 is cleaved in response to sterol depletion in fission yeast, wild-type cells were cultured in the absence or presence of compactin, a sterol synthesis inhibitor that blocks production of mevalonate by HMG-CoA reductase (Brown et al., 1978). Under these conditions, compactin treatment completely blocked ergosterol synthesis (our unpublished data). In untreated wild-type yeast, antibody to the N terminus of Sre1 specifically detected the ~110 kDa full-length Sre1 precursor and minor protein species ~70–80 kDa (Figure 2A, compare lanes 1 and 5). Treatment of cells with compactin caused a slight reduction in the level of Sre1 precursor and the appearance of cleaved N terminus of Sre1 (Sre1-N) that migrated as a broad smear from ~55–80 kDa (Figure 2A, lane 3). Proteolysis of Sre1 in response to compactin was specific insomuch as it was repressed when ergosterol synthesis was restored by addition of mevalonate, the direct product of HMG-CoA reductase (Figure 2A, lane 4). These data suggest that Sre1 is proteolytically processed in sterol-depleted cells.

Cleavage and membrane release of Sre1 by a Site-2 protease-like mechanism should produce a protein of ~50 kDa (amino acids 1–440). However, Sre1-N migrated as a smear, suggesting that Sre1-N is modified posttranslationally. The high content of serine and threonine residues in the N terminus of Sre1 (72 of first 250 residues) indicated that Sre1-N may be phosphorylated. To examine this possibility, compactin-treated protein extracts were incubated with alkaline phosphatase prior to immunoblotting. Phosphatase treatment collapsed the Sre1-N smear to a single band (Figure 2B, lane 2). Addition of EGTA inhibits the phosphatase and blocked this mobility change (Figure 2B, lane 3). Phosphatase treatment of cells grown in the absence of compactin revealed that untreated cells contain a low level of Sre1 cleavage (Figure 2B, lane 5). Phosphatase treatment had no effect on the mobility of the Sre1 precursor, suggesting that phosphorylation occurs after proteolysis.

To investigate the requirements for Sre1 cleavage, wild-type and mutant cells were grown in the absence or presence of compactin, and whole-cell extracts were immunoblotted for Sre1 before and after phosphatase treatment. As in mammalian cells, Sre1 processing required Scp1, and deletion of *scp1*$^+$ reduced the level of Sre1 precursor (Figure 2C, lanes 1 and 2 and 5 and 6) (Rawson et al., 1999). The inability to detect Sre1-N in *scp1*Δ cells was not due to reduced levels of Sre1 precursor (Figure 2C, lanes 11 and 12). Interestingly, deletion of *ins1*$^+$ or *sre2*$^+$ had no effect on Sre1 cleavage (Figure 2C, lanes 7–10), indicating that Ins1 is not essential for ER retention of Scp1 in fission yeast.

In addition to blocking sterol synthesis, compactin inhibits formation of isoprenoids used to modify prenylated proteins and to synthesize ubiquinone and heme A (Goldstein and Brown, 1990). To confirm that Sre1 cleavage resulted from reduced sterol synthesis, we assayed Sre1 cleavage in the presence of two additional ergosterol synthesis inhibitors: zaragozic acid and itraconazole. Importantly, both drugs block steps downstream of isoprenoid synthesis. Zaragozic acid inhibits squalene synthase, and itraconazole blocks demethylation of lanosterol, the first sterol in the ergosterol synthesis pathway. Treatment of wild-type yeast with zaragozic acid or itraconazole induced cleavage of Sre1 to levels seen with compactin treatment (Figure 2D, lanes 2–4), suggesting that Sre1 responded specifically to a decrease in sterol synthesis. Treatment with DMSO, the vehicle for itraconazole, had no effect on cleavage (Figure 2D, lane 5). Collectively, these data suggest that fission yeast Sre1 is activated and cleaved in response to sterol depletion by a Scp1-dependent mechanism.

Transcriptional Regulation by Sre1

Mammalian SREBPs directly regulate transcription of more than 30 genes required for cholesterol and fatty acid synthesis (Horton et al., 2003). Deletion of SCAP from mouse liver decreases transcription of HMG-CoA reductase (five times), HMG-CoA synthase (nine times), and fatty acid synthase (11 times) (Matsuda et al., 2001). To investigate whether Sre1 regulates the homologous *S. pombe* genes, we grew wild-type and mutant yeast in the absence or presence of compactin and ex-

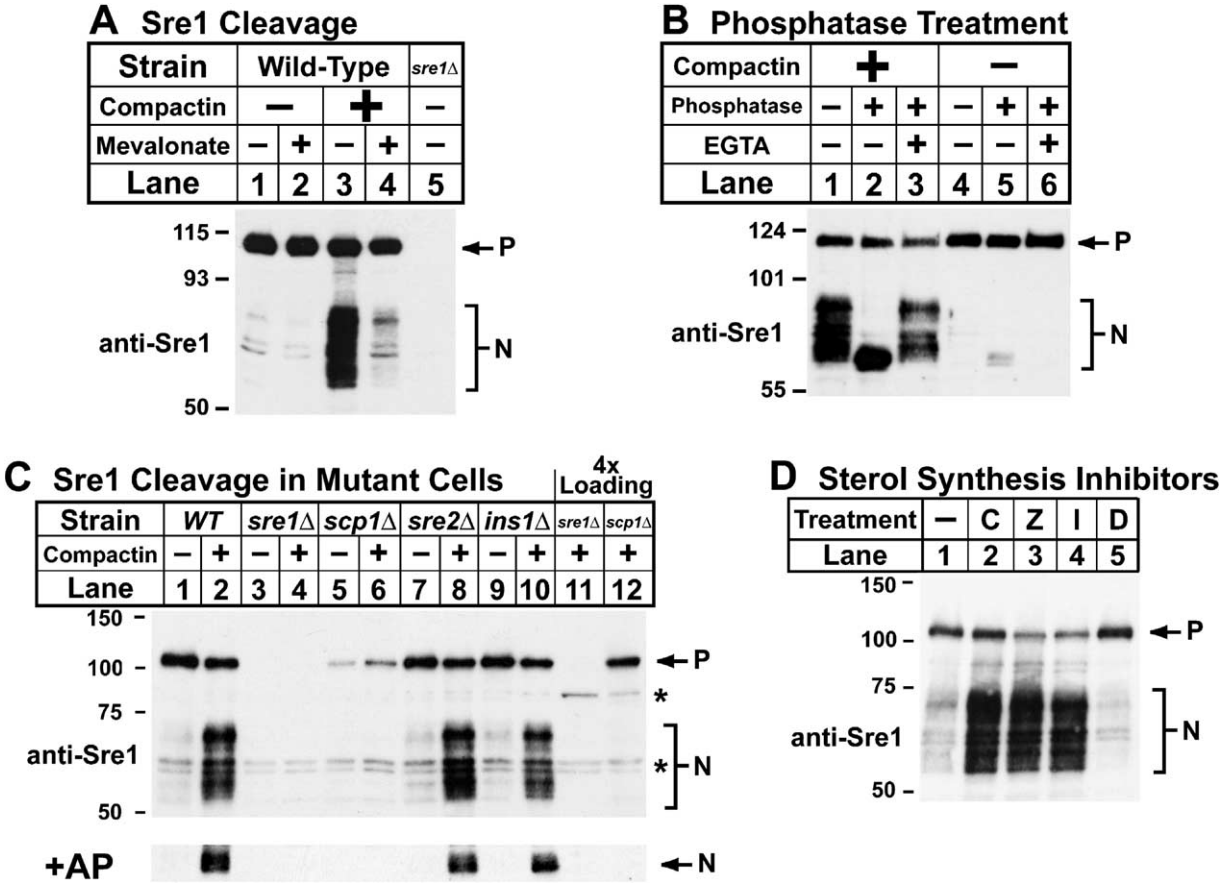

Figure 2. Sterol Depletion Activates Sre1 Cleavage

(A) Wild-type and *sre1Δ* yeast were cultured in the absence or presence of 200 μM compactin and 50 mM mevalonate for 6 hr as indicated. Whole-cell extracts were subjected to immunoblot analysis using anti-Sre1 IgG. P and N denote the precursor and cleaved nuclear forms of Sre1, respectively. Molecular mass standards (kD) are shown.

(B) Wild-type yeast were cultured in the presence (lanes 1–3) or absence (lanes 4–6) of 200 μM compactin for 6 hr. Cell extracts (10 μg of protein) were treated with alkaline phosphatase and 25 mM EGTA for 1 hr at 37°C as indicated. Treated samples were subjected to immunoblot analysis using anti-Sre1 IgG.

(C) Wild-type and mutant yeast were cultured in the absence or presence of 200 μM compactin for 6 hr as indicated. Cell extracts were subjected to immunoblot analysis using anti-Sre1 IgG before and after treatment with alkaline phosphatase (upper and lower panels, respectively). Samples in lanes 11 and 12 contain four times the amount of protein as lanes 1–10. Asterisks indicate anti-Sre1 crossreacting proteins.

(D) Wild-type yeast were grown for 6 hr in the absence or presence of ergosterol synthesis inhibitors: C, 200 μM compactin; Z, 10 μM zaragozic acid; I, 85 μM itraconazole in 0.6% DMSO; and D, 0.6% DMSO. Cell extracts were subjected to immunoblot analysis using anti-Sre1 IgG.

amined target gene expression in response to Sre1 activation. As shown previously, Sre1 was cleaved in response to sterol depletion, and cleavage required Scp1 (Figure 3, top panel). Surprisingly, expression of homologs to human HMG-CoA reductase (*hmg1*$^+$), HMG-CoA synthase (*hcs1*$^+$), and fatty acid synthase (*fas1*$^+$ and *lsd1*$^+$, the β and α subunits, respectively) was independent of sterol levels and Sre1 activity, as mRNA levels were unchanged under all conditions (Figure 3, bottom panel).

To identify physiological targets of Sre1, we performed microarray analysis using mRNA isolated from wild-type and *scp1Δ* yeast grown in the presence of compactin. This experiment allowed us to detect Sre1-dependent transcription by comparing differences in gene expression between a strain with fully activated Sre1 (Figure 3, top panel, wild-type, lane 2) and a strain with no Sre1 cleavage (Figure 3, top panel, *scp1Δ*, lane 4). Table 1 lists the ten genes whose expression showed the greatest difference between wild-type and *scp1Δ* cells. As expected, *scp1*$^+$ showed the largest change because we were comparing wild-type and *scp1Δ* strains. The genes most highly upregulated by Sre1 included the following: *hem13*$^+$, a heme biosynthetic enzyme; *scs7*$^+$ and *sur2*$^+$, two genes required for hydroxylation of sphingolipids; and, importantly, *erg3*$^+$ and *erg25*$^+$, two genes that code for enzymes acting late in the ergosterol synthesis pathway. In addition, Sre1 regulated its own expression as in mammalian cells (Horton et al., 2003). RNA expression data for *hem13*$^+$, *sre1*$^+$, and *erg3*$^+$ are shown in Figure 3 (bottom panels). Transcription of each gene increased in sterol-depleted

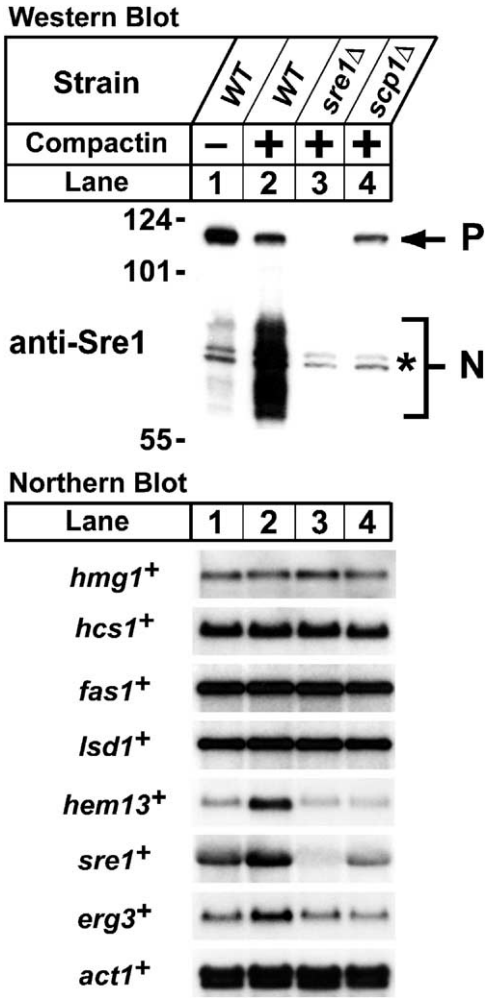

Figure 3. Sre1-Dependent Gene Transcription

Wild-type and mutant yeast were grown for 9 hr in the absence (lane 1) or presence (lanes 2–4) of 50 μM compactin. (Top panel) Cell extracts were subjected to immunoblot analysis using anti-Sre1 IgG. (Bottom panel) Total RNA was prepared from 2×10^9 cells and used for Northern blotting and DNA microarray analysis (see Table 1) as described in Experimental Procedures. Aliquots of total RNA (5 μg) were subjected to Northern blot analysis with the indicated ^{32}P-labeled probes. Unnamed *S. pombe* ORFs were assigned the gene name of the closest *S. cerevisiae* sequence homolog.

cells (Figure 3, lane 2), and this increase required activation of Sre1 (Figure 3, lanes 3 and 4). Actin (*act1*$^+$) served as a loading control. These data suggest that Sre1 functions as a transcription factor and stimulates gene expression in response to sterol depletion.

Sre1 Is Required for Anaerobic Growth

Gene deletion analysis revealed that yeast lacking *sre1*$^+$ or *scp1*$^+$ exhibit wild-type growth at a range of temperatures and on different media (our unpublished data). This result was not unexpected, since only low levels of Sre1-N are present under normal growth conditions (Figure 2B, lane 5). However, the microarray experiment suggested that Sre1 stimulated transcription of genes required in low oxygen. Five genes code for enzymes that use oxygen for their reaction mechanism, and two genes, homologs of *S. cerevisiae PFK26* and *OSM1*, are required for the shift from respiratory to fermentative growth. To examine the role of Sre1 in low oxygen growth, yeast strains were grown on rich medium in aerobic and anaerobic conditions (Figure 4A). *sre1Δ* and *scp1Δ* cells failed to grow in the absence of oxygen (Figure 4A, second panel), whereas *sre2Δ* and *ins1Δ* cells grew like wild-type. Growth of a *sre1Δ* strain was completely rescued by a plasmid expressing the active, nuclear form of Sre1 (amino acids 1–440) from a constitutive promoter (Figure 4A, Sre1-N, lower panel). In addition, Sre1-N completely rescued growth of *scp1Δ*, suggesting that, as in mammals, the essential function of Scp1 is to activate Sre1 cleavage. Transformation of an empty vector had no effect on growth. These results indicate that *sre1*$^+$ and *scp1*$^+$ are essential for anaerobic growth.

The inability of *sre1Δ* cells to grow anaerobically suggests that Sre1 may be activated under low oxygen conditions. Consistent with this hypothesis, sterol synthesis requires oxygen at multiple steps (Rosenfeld and Beauvoit, 2003), and Sre1 is cleaved in sterol-depleted cells (Figure 2). To test this prediction, wild-type and mutant yeast strains were grown in the presence or absence of oxygen for 2 hr. Protein and total RNA were isolated and subjected to immunoblot and Northern analysis. Sre1 cleavage was highly induced in the absence of oxygen (Figure 4B, upper panel, lane 2). As seen with compactin treatment, Sre1 cleavage was Scp1 dependent, and the Sre1 precursor was decreased in the absence of Scp1 (Figure 4B, upper panel, lane 4). Under low oxygen conditions, transcrip-

Table 1. Sre1-Dependent Gene Expression

S. pombe ORF	*S. pombe* Name	*S. cerevisiae* Homolog	Function[a]	Requires O_2?	Relative Expression
SPBC3B9.15c	*scp1*$^+$		SCAP ortholog	No	16.2
SPAC222.11		*HEM13*	Coproporphyrinogen (III) oxidase	Yes	5.9
SPAC30C2.02	*mmd1*$^+$	YJR070C	Mitochondrial morphology	Unknown	2.7
SPAC630.08c		*ERG25*	C-4 methyl sterol oxidase	Yes	2.5
SPAC1687.16c		*ERG3*	C-5 sterol desaturase	Yes	2.2
SPBC19C2.09	*sre1*$^+$		SREBP ortholog	No	1.8
SPAC19G12.08		*SCS7*	Fatty acid hydroxylase	Yes	1.8
SPAC222.13c		*PFK26*	6-phosphofructo-2-kinase	No	1.8
SPBC887.15c		*SUR2*	Sphingosine hydroxylase	Yes	1.8
SPAC17A2.05		*OSM1*	Fumarate reductase	No	1.8

[a] Gene function data obtained from Incyte Proteome Bioknowledge Library.

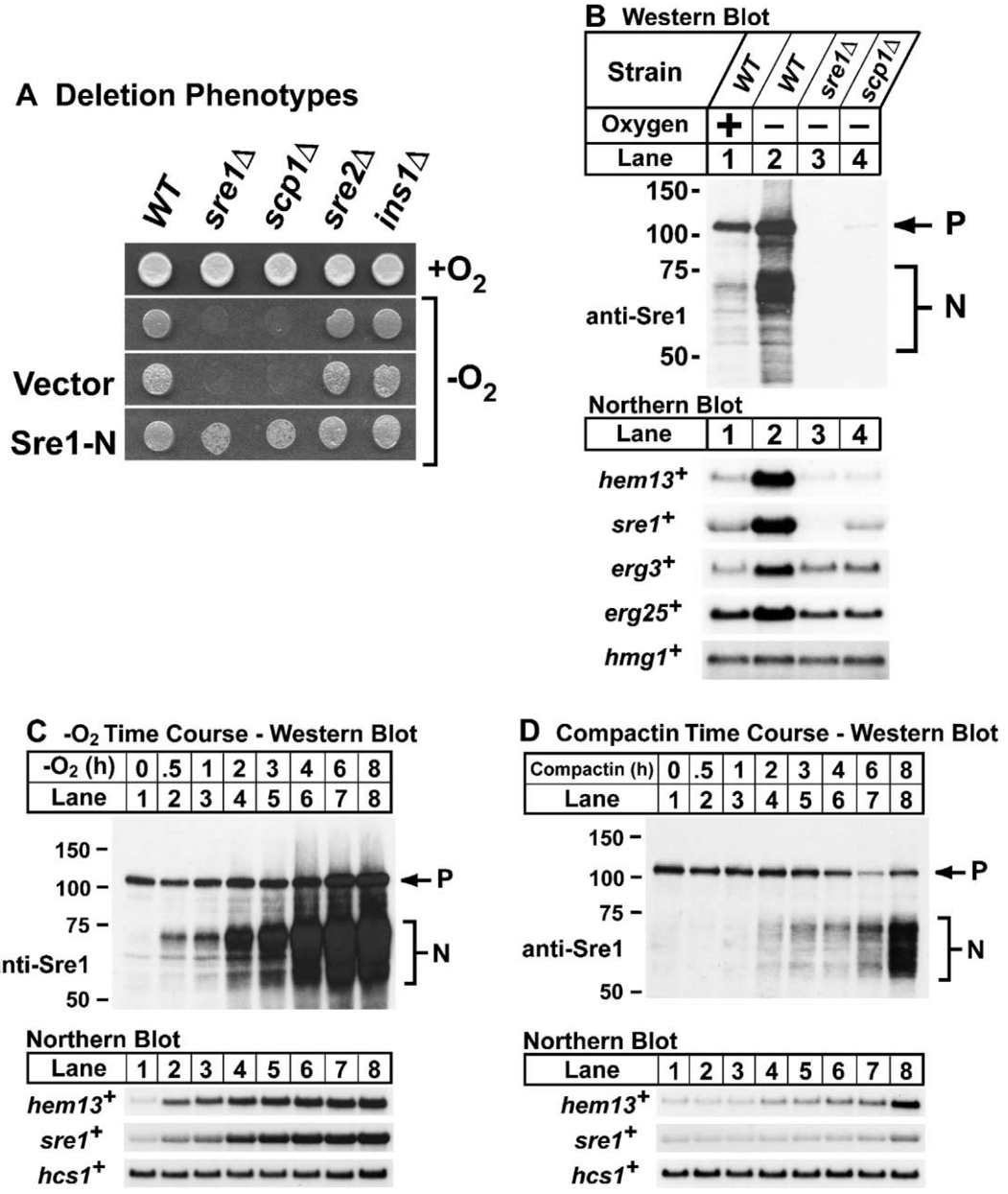

Figure 4. *sre1*$^+$ and *scp1*$^+$ Are Required for Anaerobic Growth and Gene Expression

(A) Wild-type and mutant yeast (5 × 10^3 cells) containing either no plasmid, empty vector, or a plasmid expressing Sre1-N (amino acids 1–440) from the constitutive cauliflower mosaic virus promoter were spotted on rich medium and incubated at 30°C in aerobic (top panel) or anaerobic (bottom panels) conditions for 3 or 4 days, respectively.

(B) Wild-type and mutant yeast strains were grown for 2 hr in aerobic (lane 1) or anaerobic (lanes 2–4) conditions. (Top panel) Cell extracts were subjected to immunoblot analysis using anti-Sre1 IgG. (Bottom panel) Total RNA (5 μg) was subjected to Northern blot analysis with the indicated ^{32}P-labeled probes.

(C) Wild-type yeast were shifted to anaerobic conditions at t = 0. At indicated time points, cell extracts and total RNA samples were prepared and analyzed as described in (B).

(D) Wild-type yeast were cultured in the presence of 200 μM compactin for the indicated times. Cell extracts and total RNA samples were prepared and analyzed as described in (B). Exposure times are equivalent between (C) and (D) to permit a direct comparison.

tion of *hem13*$^+$, *sre1*$^+$, *erg3*$^+$, and *erg25*$^+$ was highly upregulated in a Sre1- and Scp1-dependent manner (Figure 4B, lower panel), suggesting that Sre1 regulates the same genes under low oxygen and low sterol conditions. Transcription of *hmg1*$^+$ did not require Sre1 and served as a loading control. These data demonstrate that, in response to low oxygen, Sre1 cleavage is highly induced, leading to increased transcription of genes coding for oxygen-dependent enzymes.

To examine the kinetics of Sre1 activation under anaerobic conditions, wild-type cultures were grown in the absence of oxygen for increasing time, and sam-

ples were collected for immunoblot and Northern analysis. Figure 4C shows that Sre1 activation occurred rapidly, starting at 30 min and increasing to 8 hr (Figure 4C, upper panel). The time course for induction of *hem13*$^+$ and *sre1*$^+$ mRNA mirrored that for Sre1 activation (Figure 4C, lower panel). *hcs1*$^+$ mRNA served as a loading control. Interestingly, Sre1 precursor levels increased over time, likely due to increasing levels of *sre1*$^+$ mRNA. Given that the *S. pombe* cell cycle in these conditions is approximately 2.5 hr, these data demonstrate that Sre1 is activated in a physiological time course upon shifting to low oxygen.

To compare directly the response to low oxygen and compactin, we performed a similar experiment using wild-type cells treated with compactin. Sre1 activation occurred at 2 hr and increased to 8 hr (Figure 4D); however, the magnitude of the response was reduced dramatically when compared to anaerobic induction. Again, levels of *hem13*$^+$ and *sre1*$^+$ mRNA paralleled activation of Sre1. Unlike low oxygen, Sre1 precursor levels decreased steadily over time and then increased at 8 hr, possibly due to the delayed increase in *sre1*$^+$ mRNA. These data indicate that the cellular response to the physiological signal of low oxygen is more rapid and robust than pharmacological inhibition of sterol synthesis by compactin.

Sre1 Mediates Adaptation to Hypoxia

Collectively, our data are consistent with a role for Sre1 in adaptation to hypoxia. Figure 5A outlines a model for Sre1 function that is based on the following observations: first, Sre1 is activated in response to sterol depletion or low oxygen; second, sterol synthesis requires oxygen (Rosenfeld and Beauvoit, 2003); third, Sre1 stimulates transcription of genes coding for oxygen-dependent enzymes and genes required for a shift to fermentative growth; and fourth, sterols inhibit SREBP cleavage in mammalian cells (Wang et al., 1994). According to this model, a decrease in oxygen concentration reduces ergosterol synthesis (step 1); reduced sterol levels are then sensed by Sre1-Scp1, leading to Sre1 cleavage activation and transcription of oxygen-dependent enzymes (step 2); higher enzyme concentration increases utilization of available oxygen and synthesis of oxygen-dependent products required for continued cell growth (step 3); finally, the adaptive increase in sterol synthesis feeds back to reduce Sre1 activation (step 4). We presented evidence for step 2 in Figures 2–4. Here, we examined whether steps 1, 3, and 4 also have an experimental basis.

To test whether shifting to low oxygen decreased sterol synthesis (step 1), we assayed ergosterol synthesis during the first hour of hypoxic growth. During this period, which we refer to as unadapted hypoxia, Sre1 was not fully active (see Figure 6A, lanes 1 and 2 and 7 and 8). Wild-type yeast were labeled for 1 hr with ^{14}C-acetate in the presence of oxygen (20.9%) or immediately after shifting cells to low oxygen. After 1 hr, sterols were extracted and analyzed by thin layer chromatography. Ergosterol synthesis decreased 5-fold upon shifting cells to 0.2% oxygen and 30-fold upon shifting to anaerobic conditions (Figure 5B, lanes 1, 2, and 6). This decrease in synthesis was not due to decreased ^{14}C-acetate uptake, since overall acetate incorporation

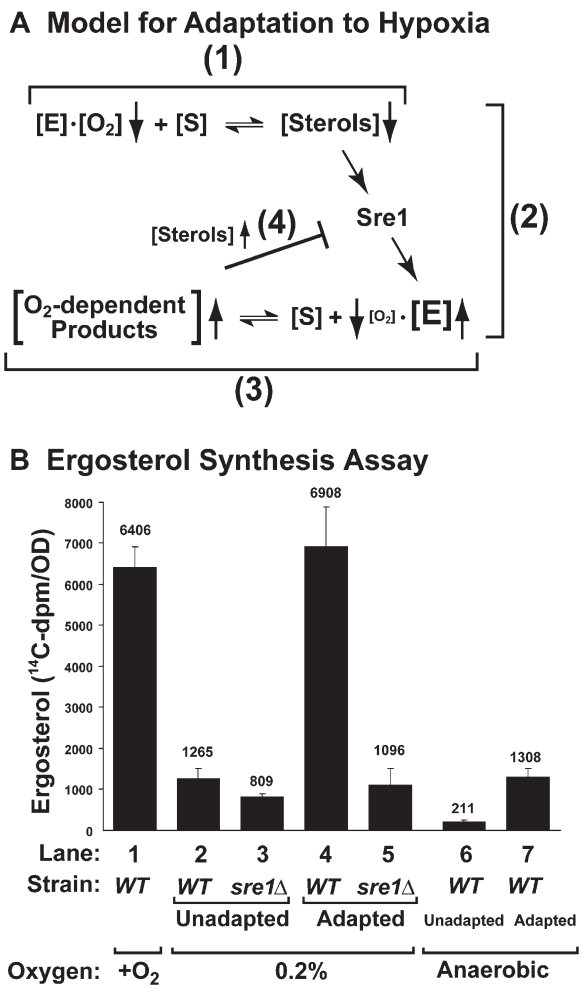

Figure 5. Model for Sre1-Regulated Adaptation to Hypoxia

(A) Sre1 and Scp1 sense sterols as an indirect measure of oxygen concentration. Step 1, reduced oxygen concentration lowers ergosterol synthesis. Step 2, sterol depletion induces cleavage and activation of Sre1, leading to increased transcription of oxygen-utilizing enzymes. Step 3, higher concentration of enzyme scavenges available oxygen by mass action, allowing synthesis of oxygen-dependent products required for continued cell growth. Step 4, increased sterol synthesis downregulates Sre1 activation. E and S denote enzyme and substrate, respectively.

(B) Wild-type and *sre1Δ* yeast were pulse labeled with ^{14}C-acetate at 30°C for 1 hr either under aerobic conditions (lane 1), immediately after shifting to low oxygen (unadapted; lanes 2, 3, and 6), or after 4 hr in low oxygen (adapted; lanes 4, 5, and 7). Low oxygen was either 0.2% oxygen (lanes 2–5) or anaerobic (lanes 6 and 7). Sterols were extracted, analyzed by thin layer chromatography (TLC), and quantified using a phosphorimager as described in Experimental Procedures. Data are the mean of six replicates from two independent experiments. Error bars equal one standard deviation. 1 OD unit = 1 × 10^7 cells.

increased in 0.2% oxygen and was unchanged anaerobically (see Figure S1 in the Supplemental Data available with this article online). This result confirms step 1 of the model and demonstrates that ergosterol synthesis decreases upon shift to low oxygen.

Step 3 of the model hypothesizes that, upon Sre1 activation, cells transition from an initial unadapted hypoxic state to a Sre1-dependent adapted state. In

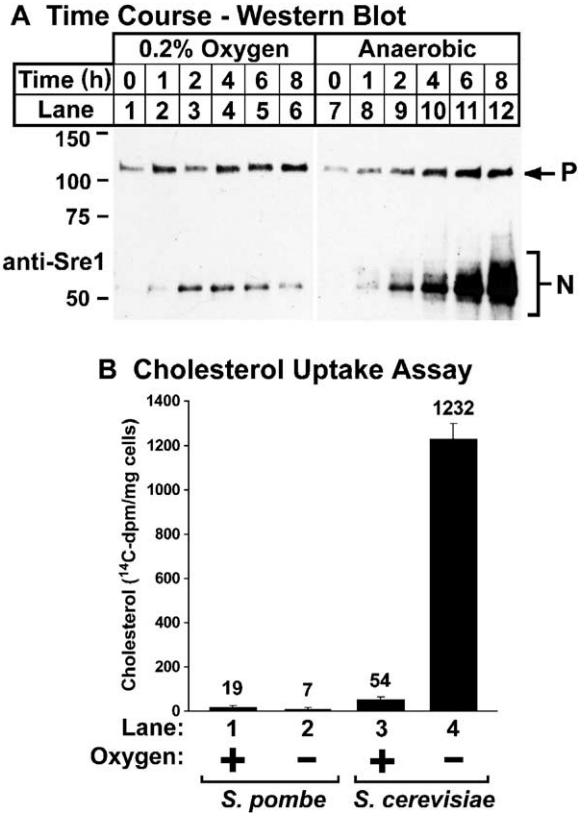

Figure 6. Feedback Inhibition of Sre1

(A) Wild-type yeast were cultured for the indicated times either in 0.2% oxygen or in anaerobic conditions. To minimize fluctuations in oxygen concentration caused by repeated entry to the workstation at 0.2% oxygen, each time point was a separate experiment performed consecutively over 3 days. The anaerobic experiment was also performed using this method. Cells extracts (10 μg) were subjected to phosphatase treatment and immunoblot analysis with anti-Sre1 IgG.

(B) Wild-type *S. pombe* and *S. cerevisiae* were incubated with 0.01 μCi/ml ^{14}C-cholesterol for 6 hr in the presence or absence of oxygen as indicated. Cholesterol uptake was measured as described in Experimental Procedures. Mean value from triplicate samples is shown above each column. Error bars equal one standard deviation.

this adapted state, Sre1 target enzyme levels are elevated, allowing cells to scavenge oxygen and synthesize oxygen-dependent products despite the hypoxic environment. Cells lacking Sre1 cannot adapt, and thus synthesis of oxygen-dependent products will remain at unadapted levels. To test this prediction, ergosterol synthesis was assayed as above in wild-type and *sre1Δ* cells either immediately after shifting cells to low oxygen (unadapted) or after 4 hr of hypoxic preconditioning (adapted). In the unadapted state, ergosterol synthesis was similar between wild-type cells and *sre1Δ* cells (Figure 5B, lanes 2 and 3), indicating that Sre1 is not required for sterol synthesis under these conditions. In the adapted state, ergosterol synthesis in wild-type cells increased 5-fold, equaling that seen under aerobic conditions (Figure 5B, lanes 1 and 4). Importantly, in *sre1Δ* cells, ergosterol synthesis was unchanged, indicating that the adaptive response required Sre1 (Figure 5B, lanes 3–5). Acetate incorporation was similar among these samples (Figure S1). These data demonstrate that Sre1 is required for an adaptive increase in ergosterol synthesis.

To test whether this adaptive increase in ergosterol synthesis leads to reduced Sre1 activation (Figure 5A, step 4), wild-type cells were cultured for increasing time either in 0.2% oxygen or anaerobic conditions. Samples were phosphatase treated prior to immunoblotting. The kinetics of Sre1 activation were similar between 0.2% oxygen and anaerobic conditions (Figure 6A). However, in 0.2% oxygen, Sre1 activation was transient, increasing by 4 hr and then decreasing by 8 hr (Figure 6A, lanes 1–6). The duration of transient Sre1 activation at 0.2% oxygen varied between experiments, likely due to instability of the hypoxic workstation (±0.1%) and resultant variations in sterol synthesis. As shown previously, under anaerobic conditions, Sre1 activation steadily increased to 8 hr (Figure 6A, lanes 7–12). This failure to reduce Sre1 activation anaerobically correlated with low levels of ergosterol synthesis in the adapted state (Figure 5B, lane 7). These data are consistent with step 4 of the model, in which feedback inhibition limits Sre1 activation under conditions of increased ergosterol synthesis.

Step 4 of the model also predicts that addition of sterols to cells should block cleavage of Sre1. However, addition of ergosterol, cholesterol, or 25-hydroxycholesterol, a potent inhibitor of mammalian SREBP cleavage (Wang et al., 1994), had no effect on Sre1 cleavage induced by compactin or low oxygen (our unpublished data). To test if the failure to suppress Sre1 cleavage was due to a defect in sterol import, we measured ^{14}C-cholesterol uptake under aerobic and anaerobic conditions. *S. pombe* failed to take up sterols under both conditions, whereas *S. cerevisiae* transported sterols specifically under anaerobic conditions to previously published levels (Figure 6B) (Wilcox et al., 2002). This phenomenon in *S. cerevisiae* is called aerobic sterol exclusion (Lorenz and Parks, 1991). Thus, unlike *S. cerevisiae*, *S. pombe* does not import exogenous cholesterol, providing an explanation for the failure of sterols to inhibit Sre1 cleavage. This finding is consistent with our model. If *S. pombe* were to import sterols under hypoxic conditions, activation of Sre1 would be suppressed, and transcription of oxygen-dependent enzymes would not increase. In this situation, cells would have a sufficient supply of sterol, but products from other oxygen-dependent reactions would be limiting. Collectively, these results support the model outlined in Figure 5A in which Sre1 and Scp1 monitor oxygen-dependent sterol synthesis as an indirect measure of oxygen supply and control adaptation to hypoxia.

Discussion

In the current study, we describe a eukaryotic oxygen-sensing mechanism that requires the SREBP pathway. Our data in fission yeast suggest that Sre1 and Scp1 monitor oxygen-dependent sterol synthesis as a measure of oxygen availability and control a transcriptional program required for adaptation to hypoxia. In this

model (Figure 5A), low oxygen decreases sterol synthesis, which in turn activates Sre1 and stimulates transcription of genes required for hypoxic growth. The resultant increase in oxygen-dependent enzymes maintains flux through reactions that may be rate limiting at low oxygen concentrations. Similar models have been proposed to explain upregulation of hypoxic genes in *S. cerevisiae* (Kwast et al., 1998). This model for Sre1-mediated adaptation to hypoxia is supported by the following evidence: (1) *sre1*$^+$ and *scp1*$^+$ are essential for anaerobic growth (Figure 4A), (2) Sre1 is cleaved in sterol-depleted cells (Figure 2), (3) low oxygen reduces sterol synthesis (Figure 5B), (4) Sre1 is activated in low oxygen (Figure 4C), (5) Sre1 activates genes required for adaptation to hypoxia (Figure 4B), and (6) Sre1 activation is required to restore aerobic levels of sterol synthesis under low oxygen conditions (Figure 5B). In this study, we measured the effects of Sre1 activation on sterol synthesis, but we speculate that other Sre1-dependent pathways such as heme and sphingolipid synthesis will respond similarly.

Cholesterol exerts feedback control on activation of SREBP in mammalian cells (Rawson, 2003), and our data are consistent with a similar role for sterols in the regulation of Sre1 in *S. pombe*. Activation of Sre1 was transient under conditions in which cells adapted to low oxygen (0.2%) and increased ergosterol synthesis (Figures 5B and 6A). However, under anaerobic conditions in which ergosterol synthesis was severely impaired, Sre1 was not downregulated. The kinetics of Sre1 activation in both conditions was rapid, suggesting that low oxygen is a physiological signal for Sre1. Interestingly, pharmacological inhibition of sterol synthesis by compactin showed a delay in Sre1 activation compared to low oxygen (Figure 4). These two treatments affect ergosterol synthesis at different points. Compactin inhibits an early step in ergosterol synthesis, whereas low oxygen affects five independent reactions late in the ergosterol pathway. Thus, compactin-treated cells may continue to synthesize ergosterol from preexisting intermediates, while hypoxic cells may experience an immediate decrease in sterol synthesis leading to more rapid Sre1 activation. Alternatively, additional oxygen-dependent mechanisms may contribute to increases in Sre1 levels. In mammalian cells, hypoxia blocks degradation of the hypoxic transcription factor HIF1-α, and a similar mechanism may act on Sre1 (Semenza, 2001).

Several lines of evidence indicate that Sre1 and Scp1 are functional orthologs of the corresponding mammalian genes. First, protein topology and key functional residues of SREBP and SCAP are conserved (Figure 1). Second, endogenous Sre1 and Scp1 form a tight complex in cells (Figure 1D), and Sre1 precursor levels are reduced in the absence of Scp1 as observed in mammalian cells. Third, Sre1 is proteolytically cleaved in response to sterol depletion through a Scp1-dependent mechanism (Figure 2). By analogy to the mammalian and *D. melanogaster* systems, Sre1 cleavage likely occurs following transport to the Golgi (Rawson, 2003). While Sre1 and Sre2 possess sequences in the predicted luminal loop that resemble the Site-1 protease consensus cleavage site (RXXL/K) (Espenshade et al., 1999), both proteins lack a sequence required for Site-2 protease cleavage (NP) in the first transmembrane segment of SREBP (Ye et al., 2000; Seegmiller et al., 2002). A clear understanding of how Sre1 is released from the membrane awaits the identification of the protease(s).

The ER resident protein Insig plays an important role in sterol regulation of SREBP cleavage. In sterol-replete mammalian cells, SCAP forms a complex with Insig, blocking ER exit and cleavage of SREBP (Yang et al., 2002). Interestingly unlike *D. melanogaster* (Rawson, 2003), *S. pombe* contains a homolog of Insig, *ins1*$^+$, and residues required for SCAP binding to Insig are conserved in Scp1. Deletion of *ins1*$^+$ had no effect on Sre1 activation, suggesting that a redundant protein or mechanism exists to regulate ER exit of Sre1/Scp1 (Figure 2C). While the function of Ins1 is unclear, the presence of each component of the SREBP pathway in fission yeast, *sre1*$^+$, *scp1*$^+$, and *ins1*$^+$, makes *S. pombe* an ideal genetic model for future studies of sterol homeostasis.

Microarray expression analysis of sterol-depleted yeast reveals that Sre1 and SREBP regulate overlapping but distinct sets of target genes (Table 1). In mammals, SREBP regulates every enzyme required for sterol biosynthesis (Horton et al., 2003), while, in *S. pombe*, Sre1 appears to activate only genes in the late sterol pathway. Furthermore, SREBP but not Sre1 regulates fatty acid synthase, and Sre1 uniquely activates genes in heme and sphingolipid synthesis (Table 1). Importantly, Sre1 also activates transcription of *pfk26*$^+$ and *osm1*$^+$, two genes involved in the transition from respiration to fermentation that occurs in limiting oxygen conditions. Collectively, these results suggest that Sre1 may play a broad role in adaptation to hypoxia.

The discovery of SREBP in fission yeast but not budding yeast suggests that *S. cerevisiae* has non-SREBP mechanisms for regulating sterol homeostasis and adaptation to hypoxia. Indeed, the *S. cerevisiae* transcription factor Upc2p stimulates expression of ergosterol biosynthetic and sterol uptake genes in sterol-depleted cells (Wilcox et al., 2002; Vik and Rine, 2001). However, Upc2p is a Zn[2]-Cys[6] binuclear cluster transcription factor with no sequence homology to SREBP (Vik and Rine, 2001). In *S. cerevisiae*, a heme-dependent mechanism regulates expression of aerobic and anaerobic genes through the activator Hap1p and repressor Rox1p (Kwast et al., 2002). Interestingly, the anaerobic expression of the Sre1-dependent genes *erg3*$^+$, *erg25*$^+$, *sur2*$^+$, *scs7*$^+$, and *hem13*$^+$ is controlled by *ROX1* in *S. cerevisiae*, suggesting that *S. pombe* and *S. cerevisiae* may regulate similar genes hypoxically albeit through different mechanisms. While Sre1 is the first mechanism of hypoxic regulation described in fission yeast, additional mechanisms may exist, such as a heme-sensing pathway similar to the *HAP1/ROX1* pathway in *S. cerevisiae*.

Importantly, fungal database searches revealed that the Sre1/Scp1 pathway is not unique to *S. pombe*. Homologs of *sre1*$^+$ and/or *scp1*$^+$ were identified in several ascomycetes, including *Aspergillus* and *Neurospora*, and the basidomycetes *Cryptococcus* and *Ustilago*. No identifiable homolog was found in *Candida*, a yeast closely related to *S. cerevisiae*, suggesting that these genes were lost from a common ancestor. Insomuch as

sre1$^+$ is required for hypoxic growth in *S. pombe*, the SREBP pathway represents a therapeutic target for pathogenic fungi that propagate in hypoxic environments.

In this study, we present data indicating that the SREBP pathway functions as an oxygen sensor and is required for adaptation to hypoxia in fission yeast. Based on these findings, we propose that SREBP and SCAP may play an unrecognized role in oxygen sensing in mammals. Unlike *S. pombe*, mammalian cells receive cholesterol from two sources: de novo synthesis and receptor-mediated endocytosis of low-density lipoprotein (LDL). Consequently, in low-oxygen conditions, LDL cholesterol should suppress SREBP activation and block induction of hypoxic genes. Therefore, we speculate that the SREBP hypoxic response may function in nonhepatic tissues that have low levels of LDL receptor or during development prior to tissue vascularization when supplies of oxygen and LDL are low. By focusing on this simple genetic model, we hope to advance our understanding of sterol- and oxygen-sensing mechanisms in mammals.

Experimental Procedures

Materials and standard methods (cDNA cloning, plasmids, antibody preparation, immunoblot analysis, and Northern blot analysis) are described in Supplemental Experimental Procedures.

Strains and Cell Culture

Wild-type haploid *S. pombe* were obtained from American Type Culture Collection, KGY425 (*h*$^-$, *his3-D1*, *leu1-32*, *ura4-D18*, *ade6-M210*) (Burke and Gould, 1994). For all experiments, yeast were grown to log phase at 30°C in Edinburgh minimal medium or YES medium (0.5% [w/v] yeast extract plus 3% [w/v] glucose and supplements, 225 μg/ml each of uracil, adenine, leucine, histidine, and lysine) (Moreno et al., 1991). Standard genetic manipulations and molecular biology techniques were performed as described (Sambrook and Russell, 2001; Alfa et al., 1993). *S. cerevisiae* strain FY833 (*MATa*, *ura3-52*, *lys2-Δ202*, *trp1-Δ63*, *his3-Δ200*, *leu2-Δ1*) (Winston et al., 1995) used for cholesterol uptake assays was a gift from Rob Jensen (Johns Hopkins University) and was cultured at 30°C in YEPD (2% peptone, 1% yeast extract, 2% glucose).

Gene Deletions and Epitope Tagging

S. pombe strains *sre1Δ*, *scp1Δ*, *sre2Δ*, and *ins1Δ*, lacking the entire open reading frame, and *scp1-Myc* were generated from wild-type haploid yeast (KGY425) by homologous recombination using established techniques (Bahler et al., 1998). Oligonucleotide sequences used to generate the PCR fragments are listed in Supplemental Data (Table S1).

Low Oxygen Culture Conditions

For plate assays, yeast grown in YES (5×10^3 cells) were spotted onto YES agar. Anaerobic growth conditions were maintained using a BBL GasPak Jar and an anaerobic system envelope (Becton Dickinson). For Sre1 hypoxic cleavage assays, cells were grown in YES and collected by centrifugation, and oxygenated medium was removed by aspiration. Cell pellets were resuspended in 5 ml of deoxygenated YES inside an Invivo$_2$ 400 hypoxic workstation (Biotrace, Inc.). Anaerobic conditions were maintained in the workstation using 10% hydrogen gas with balanced nitrogen in the presence of palladium catalyst. Deoxygenated medium was prepared by preincubation for >24 hr in the workstation. After resuspension, cultures were agitated at 30°C for indicated time, and 2×10^7 cells of log phase cultures were harvested for protein extraction and immunoblotting. For time course experiments, individual cultures were inoculated such that cell density was 1×10^7 cells/ml at harvest. Hypoxic conditions (0.2% ± 0.1% oxygen) were maintained by controlled mixing of air and nitrogen in an Invivo$_2$ 400 workstation.

Proteolytic Processing of Sre1 and Phosphatase Treatment

Yeast were grown in YES and treated as indicated in figure legends. Yeast (2×10^7 cells) were lysed by addition of 27 mM NaOH, 1% (v/v) 2-mercaptoethanol for 10 min on ice (Kornitzer et al., 1994). Total protein was precipitated with 6.4% trichloroacetic acid followed by an acetone wash. Proteins were solubilized with 100 μl of SDS lysis buffer (10 mM Tris-HCl [pH 6.8], 100 mM NaCl, 1% [w/v] SDS, 1 mM EDTA, 1 mM EGTA) plus protease inhibitors (25 μg/ml ALLN [Calbiochem], 10 μg/ml leupeptin, 2 μg/ml aprotinin, 5 μg/ml pepstatin A, 0.5 μM PMSF, 1 mM DTT) and subjected to SDS-PAGE and immunoblot analysis. Unless noted, 40 μg of total cell extract was resolved for immunoblot analysis. For phosphatase treatment, protein aliquots (30 μg) were mixed with an equal volume of 50 mM Tris-HCl (pH 8.0), 1% (w/v) SDS, 0.1% (v/v) 2-mercaptoethanol in a volume of 15 μl and boiled for 5 min. Following addition of 50 μl of 50 mM Tris-HCl (pH 8.0), samples were divided into three aliquots and treated with alkaline phosphatase (0.05 U/μl) and 25 mM EGTA as indicated for 1 hr at 37°C.

Coimmunoprecipitation

Yeast (3×10^7 cells) grown in YES were lysed using glass beads (0.5 mm, Sigma) in 50 μl NP-40 lysis buffer (50 mM HEPES [pH 7.4], 100 mM NaCl, 1.5 mM $MgCl_2$, 1% [v/v] NP-40) plus protease inhibitors. Soluble proteins were immunoprecipitated in 1 ml of lysis buffer using 5 μg of anti-Myc 9E10 monoclonal antibody and 20 μl protein G-Sepharose (Amersham). After 2 hr at 4°C, beads were collected by centrifugation. The resulting supernatant was precipitated with five volumes of cold acetone for 20 min at −20°C, followed by centrifugation at 4000 × g for 15 min. Precipitated protein was resuspended in 100 μl of SDS lysis buffer plus protease inhibitors. Bound protein was washed three times with 1 ml of NP-40 lysis buffer plus protease inhibitors before resuspension in SDS lysis buffer and immunoblot analysis.

S. pombe DNA Microarray Analysis

Data shown in Table 1 represent the average relative expression from two normalized dye reversal hybridizations using mRNA isolated from a single experiment. Total RNA was isolated from wild-type and *scp1Δ* yeast (2×10^9 cells) grown in YES containing 50 μM compactin for 9 hr at 30°C. Poly(A$^+$) mRNA was purified from 2 mg of total RNA using the Message Maker Kit (Life Technologies). Reverse transcription and fluorescent aminoallyl dye coupling reactions were performed according to manufacturer's instructions (Eurogentec). Labeled cDNA samples from the two strains were mixed and hybridized to a *S. pombe* DNA microarray slide (Eurogentec) containing 4976 ORFs spotted in duplicate. Slides were washed sequentially at RT for 5 min each with 2× SSC, 0.2% (w/v) SDS; 2× SSC; and 0.2× SSC. Slides were scanned using a GenePix 4000B scanner, and data were analyzed using GeneSpring 6 software (Silicon Genetics).

Ergosterol Synthesis Assay

To measure ergosterol synthesis, cells grown in YES were collected by centrifugation and resuspended in either oxygenated or hypoxically conditioned YES containing 2 μCi/ml ^{14}C-acetic acid sodium salt (110 mCi/mmol), such that cell density at harvest was 1×10^7 cells/ml. Cultures were then shaken at 30°C for 1 hr in normoxia, 0.2% oxygen, or anaerobically using an Invivo$_2$ 400 hypoxic workstation. To measure ergosterol synthesis during the adapted hypoxic response, cultures were grown in 0.2% oxygen or anaerobically for 4 hr prior to addition of label. After 1 hr of growth with the label, acetate uptake was halted by addition of 10 mM sodium azide. Yeast (5×10^7 cells) were collected by centrifugation, and pellets were resuspended in 9 ml of methanol followed by addition of 4.5 ml of 60% (w/v) KOH. ^{3}H-cholesterol (0.5 μCi, 40 Ci/mmol) was added to each sample as an internal standard to normalize for sterol extraction. Samples were heated to 75°C for 2 hr to saponify sterol esters. After cooling, sterols were extracted twice with 4 ml of petroleum ether. Pooled fractions were evaporated to dryness under nitrogen gas and resuspended in 200 μl of hexane. Five microliters of each sample was used to analyze ^{3}H-cholesterol recovery by scintillation counting. Samples were then concentrated using nitrogen gas to a final volume of 25 μl and applied to Silica

Gel 60 F_{254} plates (EMD Chemicals, Inc.). TLC was performed as previously described (Gardner et al., 2001). ^{14}C-labeled lipids were detected by autoradiography using a Personal FX Molecular Imaging System (Biorad). Relative intensities of lipids on all plates were converted to ^{14}C-dpm by direct comparison to a standard curve of known ^{14}C-cholesterol concentrations. Sterol species were identified by direct comparison to known standards visualized by iodine vapor.

Cholesterol Uptake Assay

To measure cholesterol uptake, *S. cerevisiae* and *S. pombe* cells grown in YEPD or YES, respectively, were collected and resuspended in appropriate oxygenated or deoxygenated medium containing 0.01 μCi/ml ^{14}C-cholesterol (55 mCi/mmol) and 1% tyloxapol:ethanol (1:1, v/v). Cultures were grown with shaking at 30°C for 6 hr aerobically or anaerobically in an Invivo$_2$ hypoxic workstation such that cell density at harvest was 2 × 10^7 cells/ml. After 6 hr, 1 × 10^8 cells were collected by vacuum filtration onto preweighed 0.45 μm HV Durapore membrane filters (Millipore). Cells were washed twice with 0.5% tergitol (v/v) and once with water, after which filters were dried and weighed. Total cholesterol incorporation was measured by scintillation counting, and final uptake values were expressed as ^{14}C-cholesterol-dpm/mg cell weight.

Supplemental Data

Supplemental Data include one figure, one table, Supplemental Experimental Procedures, and Supplemental References and are available with this article online at http://www.cell.com/cgi/content/full/120/6/831/DC1/.

Acknowledgments

From UT-Southwestern Medical Center at Dallas, we are deeply grateful to Dr. Joseph Goldstein and Dr. Michael Brown for their expert guidance and training. We thank Norma Anderson, Tammy Dinh, and Richard Gibson for excellent technical assistance. From Johns Hopkins, we thank Raymond Chai and Anuradha Gokhale for outstanding technical assistance. This work was supported by a grant from the National Insitutes of Health (HL-077588) (to P.E.). A.L.H. and B.L.T. are supported by NIH training grant GM007445. P.J.E. is a recipient of a Burroughs Wellcome Fund Career Award in the Biomedical Sciences.

Received: July 20, 2004
Revised: November 2, 2004
Accepted: January 19, 2005
Published: March 24, 2005

References

Alfa, C., Fantes, P., Hyams, J., McLeod, M., and Warbrick, E. (1993). Experiments with Fission Yeast: A Laboratory Course Manual (Cold Spring Harbor: New York).

Bahler, J., Wu, J.Q., Longtine, M.S., Shah, N.G., McKenzie, A., Steever, A.B., Wach, A., Philippsen, P., and Pringle, J.R. (1998). Heterologous modules for efficient and versatile PCR-based gene targeting in *Schizosaccharomyces pombe*. Yeast *14*, 943–951.

Brown, M.S., Faust, J.R., Goldstein, J.L., Kaneko, I., and Endo, A. (1978). Induction of 3-hydroxy-3-methylglutaryl coenzyme-A reductase-activity in human fibroblasts incubated with compactin (ML-236B), a competitive inhibitor of reductase. J. Biol. Chem. *253*, 1121–1128.

Burke, J.D., and Gould, K.L. (1994). Molecular cloning and characterization of the *Schizosaccharomyces pombe* his3 gene for use as a selectable marker. Mol. Gen. Genet. *242*, 169–176.

DeBose-Boyd, R.A., Brown, M.S., Li, W.P., Nohturfft, A., Goldstein, J.L., and Espenshade, P.J. (1999). Transport-dependent proteolysis of SREBP: relocation of Site-1 protease from Golgi to ER obviates the need for SREBP transport to Golgi. Cell *99*, 703–712.

Dobrosotskaya, I.Y., Seegmiller, A.C., Brown, M.S., Goldstein, J.L., and Rawson, R.B. (2002). Regulation of SREBP processing and membrane lipid production by phospholipids in *Drosophila*. Science *296*, 879–883.

Espenshade, P.J., Cheng, D., Goldstein, J.L., and Brown, M.S. (1999). Autocatalytic processing of site-1 protease removes propeptide and permits cleavage of sterol regulatory element-binding proteins. J. Biol. Chem. *274*, 22795–22804.

Feramisco, J.D., Goldstein, J.L., and Brown, M.S. (2004). Membrane topology of human Insig-1, a protein regulator of lipid synthesis. J. Biol. Chem. *279*, 8487–8496.

Gardner, R.G., Shan, H., Matsuda, S.P., and Hampton, R.Y. (2001). An oxysterol-derived positive signal for 3-hydroxy-3-methylglutaryl-CoA reductase degradation in yeast. J. Biol. Chem. *276*, 8681–8694.

Goldstein, J.L., and Brown, M.S. (1990). Regulation of the mevalonate pathway. Nature *343*, 425–430.

Horton, J.D., Goldstein, J.L., and Brown, M.S. (2002). SREBPs: activators of the complete program of cholesterol and fatty acid synthesis in the liver. J. Clin. Invest. *109*, 1125–1131.

Horton, J.D., Shah, N.A., Warrington, J.A., Anderson, N.N., Park, S.W., Brown, M.S., and Goldstein, J.L. (2003). Combined analysis of oligonucleotide microarray data from transgenic and knockout mice identifies direct SREBP target genes. Proc. Natl. Acad. Sci. USA *100*, 12027–12032.

Hua, X.X., Yokoyama, C., Wu, J., Briggs, M.R., Brown, M.S., Goldstein, J.L., and Wang, X.D. (1993). SREBP-2, a second basic-helix-loop-helix-leucine zipper protein that stimulates transcription by binding to a sterol regulatory element. Proc. Natl. Acad. Sci. USA *90*, 11603–11607.

Kornitzer, D., Raboy, B., Kulka, R.G., and Fink, G.R. (1994). Regulated degradation of the transcription factor Gcn4. EMBO J. *13*, 6021–6030.

Kwast, K.E., Burke, P.V., and Poyton, R.O. (1998). Oxygen sensing and the transcriptional regulation of oxygen-responsive genes in yeast. J. Exp. Biol. *201*, 1177–1195.

Kwast, K.E., Lai, L.C., Menda, N., James, D.T., III, Aref, S., and Burke, P.V. (2002). Genomic analyses of anaerobically induced genes in *Saccharomyces cerevisiae*: functional roles of Rox1 and other factors in mediating the anoxic response. J. Bacteriol. *184*, 250–265.

Loewen, C.J., and Levine, T.P. (2002). Cholesterol homeostasis: not until the SCAP lady INSIGs. Curr. Biol. *12*, R779–R781.

Lorenz, R.T., and Parks, L.W. (1991). Involvement of heme components in sterol metabolism of *Saccharomyces cerevisiae*. Lipids *26*, 598–603.

Matsuda, M., Korn, B.S., Hammer, R.E., Moon, Y.A., Komuro, R., Horton, J.D., Goldstein, J.L., Brown, M.S., and Shimomura, I. (2001). SREBP cleavage-activating protein (SCAP) is required for increased lipid synthesis in liver induced by cholesterol deprivation and insulin elevation. Genes Dev. *15*, 1206–1216.

McKay, R.M., McKay, J.P., Avery, L., and Graff, J.M. (2003). *C. elegans*: a model for exploring the genetics of fat storage. Dev. Cell *4*, 131–142.

Moreno, S., Klar, A., and Nurse, P. (1991). Molecular genetic analysis of fission yeast *Schizosaccharomyces pombe*. Methods Enzymol. *194*, 795–823.

Parraga, A., Bellsolell, L., Ferre-D'Amare, A.R., and Burley, S.K. (1998). Co-crystal structure of sterol regulatory element binding protein 1a at 2.3 Å resolution. Structure *6*, 661–672.

Rawson, R.B. (2003). The SREBP pathway–insights from Insigs and insects. Nat. Rev. Mol. Cell Biol. *4*, 631–640.

Rawson, R.B., DeBose-Boyd, R., Goldstein, J.L., and Brown, M.S. (1999). Failure to cleave sterol regulatory element-binding proteins (SREBPs) causes cholesterol auxotrophy in Chinese hamster ovary cells with genetic absence of SREBP cleavage-activating protein. J. Biol. Chem. *274*, 28549–28556.

Rosenfeld, E., and Beauvoit, B. (2003). Role of the non-respiratory pathways in the utilization of molecular oxygen by *Saccharomyces cerevisiae*. Yeast *20*, 1115–1144.

Sambrook, J., and Russell, D.W. (2001). Molecular Cloning: A Laboratory Manual (Cold Spring Harbor: New York).

Seegmiller, A.C., Dobrosotskaya, I., Goldstein, J.L., Ho, Y.K., Brown, M.S., and Rawson, R.B. (2002). The SREBP pathway in *Drosophila*: regulation by palmitate, not sterols. Dev. Cell *2*, 229–238.

Semenza, G.L. (2001). HIF-1 and mechanisms of hypoxia sensing. Curr. Opin. Cell Biol. *13*, 167–171.

Smith, T.F., Gaitatzes, C., Saxena, K., and Neer, E.J. (1999). The WD repeat: a common architecture for diverse functions. Trends Biochem. Sci. *24*, 181–185.

Vik, A., and Rine, J. (2001). Upc2p and Ecm22p, dual regulators of sterol biosynthesis in *Saccharomyces cerevisiae*. Mol. Cell. Biol. *21*, 6395–6405.

Wang, X.D., Sato, R., Brown, M.S., Hua, X.X., and Goldstein, J.L. (1994). SREBP-1, a membrane-bound transcription factor released by sterol-regulated proteolysis. Cell *77*, 53–62.

Wilcox, L.J., Balderes, D.A., Wharton, B., Tinkelenberg, A.H., Rao, G., and Sturley, S.L. (2002). Transcriptional profiling identifies two members of the ATP-binding cassette transporter superfamily required for sterol uptake in yeast. J. Biol. Chem. *277*, 32466–32472.

Winston, F., Dollard, C., and Ricupero-Hovasse, S.L. (1995). Construction of a set of convenient *Saccharomyces cerevisiae* strains that are isogenic to S288C. Yeast *11*, 53–55.

Yabe, D., Xia, Z.P., Adams, C.M., and Rawson, R.B. (2002). Three mutations in sterol-sensing domain of SCAP block interaction with insig and render SREBP cleavage insensitive to sterols. Proc. Natl. Acad. Sci. USA *99*, 16672–16677.

Yang, T., Espenshade, P.J., Wright, M.E., Yabe, D., Gong, Y., Aebersold, R., Goldstein, J.L., and Brown, M.S. (2002). Crucial step in cholesterol homeostasis: Sterols promote binding of SCAP to INSIG-1, a membrane protein that facilitates retention of SREBPs in ER. Cell *110*, 489–500.

Ye, J., Dave, U.P., Grishin, N.V., Goldstein, J.L., and Brown, M.S. (2000). Asparagine-proline sequence within membrane-spanning segment of SREBP triggers intramembrane cleavage by Site-2 protease. Proc. Natl. Acad. Sci. USA *97*, 5123–5128.